TURBULENT STATISTICS OF RAREFIED FLOWS IN A MICROCHANNEL

Dong-Xing Du, Kenjiro Suzuki
Department of Mechanical Engineering,
Kyoto University
Yoshida-Honmachi, Sakyo-ku, Kyoto 606-8501, Japan
dxdu@mech.kyoto-u.ac.jp, ksuzuki@mech.kyoto-u.ac.jp

ABSTRACT

Direct Numerical Simulation (DNS) has been carried out to investigate the effect of weak rarefaction on turbulent flow characteristics in microchannels. Knudsen numbers of the simulated flow are selected to be 0.0(un-rarefied), 0.001, 0.005, 0.01 and 0.02 respectively. Validity of the calculation is demonstrated by the combination of presenting the data of two-point correlation functions and one-dimensional power spectra and comparing the results with available reported results. Turbulent statistics including mean streamwise velocity, turbulent intensities and Reynolds shear stress are investigated under the rarefied conditions. It can be concluded that the weakly rarefied turbulent flow has higher streamwise velocity over the whole channel width. Rarefaction can also lead to higher turbulent intensities and higher Reynolds shear stress in the vicinity of the wall.

INTRODUCTION

In relation with the rapidly expanding application of micro scale devices in industries, momentum and heat transfer in micro channels becomes an important research subject. However, there exists inconsistency among the reported experimental data on the friction coefficient measured in the micro-channels. Some data show the decrease of the friction coefficient (Pfahler et al. 1990,1991; Choi et al. 1991; Harley et al. 1995; Araki et al. 2002), but others show the opposite direction of the change (Wu and Little, 1983; Mala and Li, 1999; Du et al. 2000). These inconsistent results indicate the necessity of detailed studies for the fluid flow in micro-channels.

Rarefaction effect is an important influential factor that must be taken into consideration in the study of micro-scale fluid flow and heat transfer (Pfahler et al. 1991; Choi et al. 1991; Pong et al. 1994; Harley et al. 1995; Beskok et al. 1996; Arkilic et al. 1997; Kavehpour et al. 1997; Beskok and Karniadakis, 1999; Araki et al. 2002). Rarefied flows can be characterized by the Knudsen number Kn, defined by $Kn = \lambda / L$, where λ is the mean-free-path of fluid molecules and L is a characteristic length of a system. The value of Knudsen number reflects the degree of rarefaction and therefore determines the conditions where the continuum model holds. Four different flow regimes can be identified with the value of Knudsen number as follows (Tsien, 1946):

- Continuum flow regime: $Kn < 10^{-3}$
- Slip flow (slightly rarefied) regime: $10^{-3} < Kn < 10^{-1}$
- Transitional regime: $10^{-1} < Kn < 10$
- Free molecular flow regime: $Kn > 10$

The breakdown of the continuum approximation occurs at $Kn > 0.001$. On the other hand, Knudsen number can be rewritten as $Kn \approx M / \mathrm{Re}$, where M is the Mach number, and Re is the Reynolds number of the flow. Based on the suggestions reported in the references that the transition from laminar to turbulence can occur at the Reynolds number as low as 350~900 (Wu and Little, 1983) and supersonic flows can be realized in micronozzles (Ayon et al. 2001), turbulent flows in the slip flow regime can be established in a small size channel. However, up to now, no literatures have been found yet on scrutinizing the rarefied turbulent flows in microchannels.

The present study aims at studying the behavior of gaseous turbulent flows in slip flow regime. For such kind of flows, it is popularly accepted that Navier-Stokes equations are still valid but slip boundary conditions should be introduced to account for the effect of rarefaction. In this paper, direct numerical simulation is made for the slightly rarefied turbulent flows in a parallel channel and the particular study is made on how the turbulent statistics are affected by the introduction of slip velocity at the wall boundary. The flow is treated in this study to be locally incompressible and rarefaction progressing in the computational domain is treated negligible.

COMPUTATIONAL DETAILS

The computational domain and coordinate system adopted are shown in Fig. 1, where L_x, L_y, L_z are set to be $2.5\pi\delta$, 2δ and $1.0\pi\delta$ (δ the half height of the channel) respectively. Flow is supposed to be fully developed so that it is statistically homogeneous both in streamwise and spanwise directions. Periodic boundary conditions are therefore used both at streamwise and spanwise boundaries.

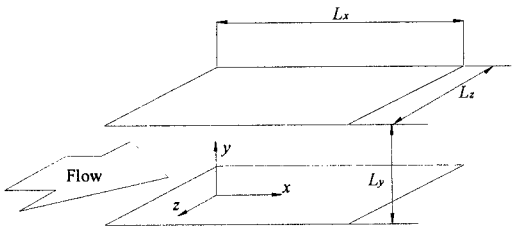

Fig.1. Computational domain

Governing equations are the mass and momentum conservation equations for incompressible fluid flow. With the friction velocity u_τ as the reference velocity and the viscous lengthscale δ_ν as the reference lengthscale, they can be written in non-dimensional forms as follows,

$$\frac{\partial U^+}{\partial x^+}+\frac{\partial V^+}{\partial y^+}+\frac{\partial W^+}{\partial z^+}=0 \tag{1}$$

$$\frac{\partial U^+}{\partial t^+}+U^+\frac{\partial U^+}{\partial x^+}+V^+\frac{\partial U^+}{\partial y^+}+W^+\frac{\partial U^+}{\partial z^+}=-\frac{\partial P^+}{\partial x^+}+\nabla^2U^+ +\frac{F}{\mathrm{Re}_\tau} \tag{2}$$

$$\frac{\partial V^+}{\partial t^+}+U^+\frac{\partial V^+}{\partial x^+}+V^+\frac{\partial V^+}{\partial y^+}+W^+\frac{\partial V^+}{\partial z^+}=-\frac{\partial P^+}{\partial y^+}+\nabla^2V^+ \tag{3}$$

$$\frac{\partial W^+}{\partial t^+}+U^+\frac{\partial W^+}{\partial x^+}+V^+\frac{\partial W^+}{\partial y^+}+W^+\frac{\partial W^+}{\partial z^+}=-\frac{\partial P^+}{\partial z^+}+\nabla^2W^+ \tag{4}$$

where Re_τ the Reynolds number based on friction velocity, or friction Reynolds number, F/Re_τ the pressure gradient to drive the flow and the value of F equals to unity under the adopted normalization.

Rarefaction effects are taken into consideration by employing the following slip flow conditions for the velocity components in x and z directions (Kennard, 1938),

$$U^+\Big|_{wall}=\sigma K_n\,\mathrm{Re}_\tau\frac{\partial U^+}{\partial y^+}\Big|_{wall} \tag{5}$$

$$W^+\Big|_{wall}=\sigma K_n\,\mathrm{Re}_\tau\frac{\partial W^+}{\partial y^+}\Big|_{wall} \tag{6}$$

where σ represents the momentum accommodation factor. As is popularly accepted in various engineering applications, σ is assumed to be unity here.

Table 1: Computational conditions.

	Kn= 0.0	Kn= 0.001	Kn= 0.005	Kn= 0.01	Kn= 0.02
Re_τ	150				
L_x/δ	7.85 (2.5π)				
L_z/δ	3.14 (1.0π)				
Grid numbers	$64\times127\times64$ (in x, y, z)				
Δx^+	18.4				
Δy^+	0.170-9.24				
Δz^+	7.36				
Δt^+	6×10^{-2}	7.5×10^{-3}			
Average time span	4800	4500	4500	4500	4500

For simplicity, superscript + will be dropped for non-dimensional velocity components and non-dimensional pressure hereafter in the text and figures. Therefore, in later discussions, U, V, W stand for non-dimensional instantaneous velocity in x, y, z directions, respectively, and P represents the non-dimensional fluctuating part of the pressure. $<U>$, $<V>$, $<W>$ denote the time mean values of U, V, W, respectively, and u, v, w represent the fluctuating part of U, V, W, respectively.

Computation code is written with the finite volume method (Matsubara et al. 1998). Computations are carried out on a staggered grid system for a frictional Reynolds number of 150. Grid points in x-, y-, z- directions are 64, 127, 64 and the dimensionless gird spacing in x- and z- directions are 18.4 and 7.36 respectively. Non-uniform meshes are used in the transverse direction with the minimum spacing of 0.17 for the first grid point away from the wall and the maximum spacing of 9.24 at the centerline of the channel.

For the numerical procedure, fractional time step or time splitting method (Kim and Moin, 1985) was employed for the time dependent term of N-S equations. Implicit Crank-Nicolson scheme was applied for the viscous term and explicit Adams-Bashforth scheme was applied for other terms. All spatial derivatives in N-S equations were discretized with fourth-order central difference scheme.

Computation was conducted under five different Knudsen numbers, that is, Kn=0.0 (normal or un-rarefied case), 0.001, 0.005, 0.01 and 0.02. Statistical results are obtained by averaging the instantaneous data over the time span of about 4500. Detailed computational conditions are listed in Table 1, where smaller time step was used in the rarefied flow cases to enhance the numerical stability.

VALIDATION

Examples of two-point correlations and energy spectra at the location of $y^+ = 5.1$ are shown in Fig. 2 and Fig. 3 to illustrate the adequacy of the computational domain and the grid resolutions. To make the figures clear to read, only the data under Kn=0.0 and Kn=0.01 are presented.

In Figs. 2(a) and 2(b), the two-point correlations in the x- and z- directions show that they fall off to values close enough to zero for the largest separations, indicating that the size of the computational domain is sufficiently large. In Figs. 3(a) and 3(b), the energy spectra in streamwise and spanwise directions are plotted separately, where k_x and k_z are the wavenumbers in x- and z- directions, respectively. It can be concluded that the grid resolution is adequate for the computation, since the energy density associated with the high wavenumbers is several order of magnitude lower than that corresponding to low wavenumbers, and there is no obvious energy pile-up at high wavenumbers.

For the validation of the accuracy of the present calculation, DNS database of Kasagi et al. (1992) for an un-rarefied turbulent channel flow of $Kn = 0.0$ is used as a reference for comparison. In the computation for the database, the pseudospectral formulation of the momentum equations is implemented, therefore, the numerical quality of the database is believed to be high enough to use as a reference. Figures. 4(a) and 4(b) show the transverse profile of the streamwise time-mean velocity $<U>$ and the square root values of the three components of Reynolds normal stresses ($u_{rms} =< u^2 >^{1/2}$) obtained for the normal case of $Kn = 0.0$ with the equivalent database of Kasagi et al. The present results obtained with the finite difference approach allocating the above mentioned in-excessive number of grid points agree quite well with Kasagi's data, which justifies the validity of the present calculation.

RESULTS AND DISCUSSION

Streamwise Mean Flow Velocity

Figure 5 shows the transverse profiles of streamwise mean-velocity, $<U>$, for all the cases of different level of rarefaction or different Knudsen numbers. Illustration is made separately for the near wall region $0 \le y^+ < 30$ in (a) and for the outer region $30 \le y^+ \le 150$ in (b), respectively. It is found that rarefaction shows its effect throughout the whole channel width, where the increase of the Knudsen number accompanies the increase of the streamwise time-mean velocity or the increase of flow rate. In other words, keeping the flow rate, friction loss becomes smaller as the effect of rarefaction. The relationship between $<U>$ and y^+ remains nearly linear for all the computational conditions in the region of $y^+ < 5$, whereas in the region of $5 < y^+ < 30$, the relationship deviates from linearity a little by little toward the core region and difference in the mean velocity among the cases of different values of Knudsen number also decreases gradually. In the core region of $y^+ > 30$, difference in the streamwise velocity related to the difference of Knudsen number distributes almost uniformly.

Turbulence Intensities

Figure 6 illustrates the transverse distribution of square root values of the three components of Reynolds normal stresses. Illustration is made again separately for two regions, $0 \le y^+ < 20$ and $20 \le y^+ \le 150$, respectively. It is clearly seen that higher Knudsen number leads to higher values of u_{rms} and w_{rms} in the near-wall region of $y^+ < 15$. The values of u_{rms} and w_{rms} are no longer zero at the wall and can reach as high as 0.9 and 0.3 under the rarefied condition of $Kn = 0.02$. The result can be attributed to the smaller restriction of the wall or the introduction of slip flow boundary conditions. However, the effect of rarefaction on u_{rms} and w_{rms} diminishes outward. Though the values of v_{rms} are zero on the wall under all computational conditions, they have slightly higher values in the region of $0 < y^+ < 50$ for higher Knudsen numbers.

Reynolds Shear Stress

Figure 7 presents the transverse distributions of the Reynolds shear stress $< -uv >$ under different Knudsen numbers. Also shown in this figure are the total shear stress $< -uv > + \tau_{xy}$, where τ_{xy} is the viscous shear stress and is defined as $\tau_{xy} = \partial < U > / \partial y^+$. Again, the results are illustrated in two separate figures, one for $0 \le y^+ < 30$ and another for $30 \le y^+ \le 150$, respectively. It is reasonable to see that the total shear stress takes in every case the value of unity at the wall and that its distribution does not vary with the change in the Knudsen number. This is because the friction acting on the wall should remain unchanged with the change of the Knudsen number when friction Reynolds number is fixed constant. However, the Reynolds shear stress becomes larger and thereby the viscous shear stress becomes smaller for higher Knudsen numbers in the near wall region of $0 < y^+ < 30$. The latter suggests that rarefaction plays an important role in this region, where velocity gradient decreases while the velocity itself increases with an increase of the Knudsen number as pointed out in the above.

CONCLUSION

DNS was carried out to study the effect of rarefaction on the turbulent flow behavior in a microchannel. Statistical characteristics studied in this paper are streamwise mean velocities, turbulent intensities and Reynolds shear stress. It can be concluded that,

1) Rarefaction can lead to higher streamwise mean velocity throughout the channel;

2) Rarefaction effect on the turbulent intensities is noticeable in the near wall region. Higher values of u_{rms} and w_{rms} are observed in the cases of higher Knudsen numbers in the region of $y^+ < 15$, while slightly higher values of v_{rms} are observed in a wider transverse range of $0 < y^+ < 50$ for rarefied flows.

3) The total shear stress remains unchanged regardless to the degree of rarefaction if the friction Reynolds number is kept constant. However, higher values of Reynolds shear stress and thereby lower values of viscous shear stress occur in the near wall region of $0 < y^+ < 30$ by the introduction of slip flow boundary conditions.

ACKNOWLEDGEMENT

This work is supported by the Japan Society for the Promotion of Science (JSPS).

REFERENCES

Araki, T., Kim, M. S., Iwai, H., and Suzuki, K., 2002, "An experimental investigation of gaseous flow characteristics in microchannels", *Microscale Thermophysical Engineering*, Vol.6, pp.117-130.

Arkilic, E. B., Schmidt, M. A., and Breuer, K. S., 1997, "Gaseous slip flow in long microchannels", *Journal of Microelectromechanical systems*, Vol.6, pp.167-178.

Ayon, A. A., Bayt, R. L., and Breuer, K. S., 2001, "Deep reactive ion etching: a promising technology for micro- and nanosatellites", *Smart Materials & Structures* Vol.10, pp.1135-1144.

Beskok, A., Karniadakis, G. E., and Trimmer, W., 1996, "Rarefaction and compressibility effects in gas microflows", *Journal of Fluid Engineering*, Vol.118, pp.448-456.

Beskok, A., and Karniadakis, G. E., 1999, "A model for flows in channels, pipes, and ducts at micro and nano scales", *Microscale thermophysical Engineering*, Vol.3, pp.43-77.

Choi, S. B., Barron, R. F., and Warrington, R. Q., 1991, "Fluid flow and heat transfer in microtubes", ASME DSC-32, pp.123-133.

Du, D. X., Li, Z. X., and Guo, Z. Y., 2000, "Friction resistance for gas flow in smooth microtubes", *Science in China-series E*, Vol.43, pp.171-177.

Harley, J. C., Huang, Y. F., Bau, H. H., and ZEMEL, J. N., 1995, "Gas flow in micro-channels", *Journal of Fluid Mechanics*, Vol. 284, pp.257-274.

Kasagi, N., Horiuti, K., Miyake, Y., Miyauchi, T., and Nagano, Y., 1992, The database and its specification is downloadable from the website of Turbulence and the Heat Transfer Laboratory, Tokyo University, http://www.thtlab.t.u-tokyo.ac.jp/index-j.html, with the DNS Database, #Code Number: CH12__PG.WL1.

Kavehpour, H. P., Faghri, M., and Asako, Y., 1997, "Effects of compressibility and rarefaction on gaseous flows in microchannels", *Numerial Heat Transfer, Part A*, Vol.32, pp.677-696.

Kennard, E. H., 1938, "Kinetic theory of Gases", New York: McGraw-Hill.

Kim, J., and Moin, P., 1985, "Application of a fractional-step method to incompressible Navier-Stokes equations", *Journal of Computational Physics*, Vol.59, pp.308-323.

Mala, G. M., and Li, D. Q., 1999, "Flow characteristics of water in microtubes", *International Journal of Heat and Fluid Flow*, Vol.20, pp.142-148.

Matsubara, K., Kobayashi, M., and Maekawa, H., 1998, "Direct numerical simulation of a turbulent channel flow with a linear spanwise mean temperature gradient", *International Journal of Heat and Mass Transfer*, Vol. 41, pp.3627-3634.

Pfahler, J., Harley, J., and Bau, H., 1990, "Liquid and gas transport in small channels", ASME DSC-19, pp.149-157.

Pfahler, J., Harley, J., and Bau, H., 1991, "Gas and liquid flow in small channels", ASME DSC-32, pp.49-60.

Pong, K. C., Ho, C. M., Liu, J., and Tai, Y. C., 1994, "Non-linear pressure distribution in uniform microchannels", ASME FED-197, pp. 51-56.

Tsien, Hsue-Shen, 1946, "Superaerodynamics, the mechanics of rarefied gases", *Journal of Aeronautical Science*, Vol.13, pp.653-664.

Wu, P. Y., and Little, W. A., 1983, "Measurement of friction factors for the flow of gases in very fine channels used for microminiature Joule-Thompson Refrigerators", *Cryogenics*, Vol.23, pp.273-277.

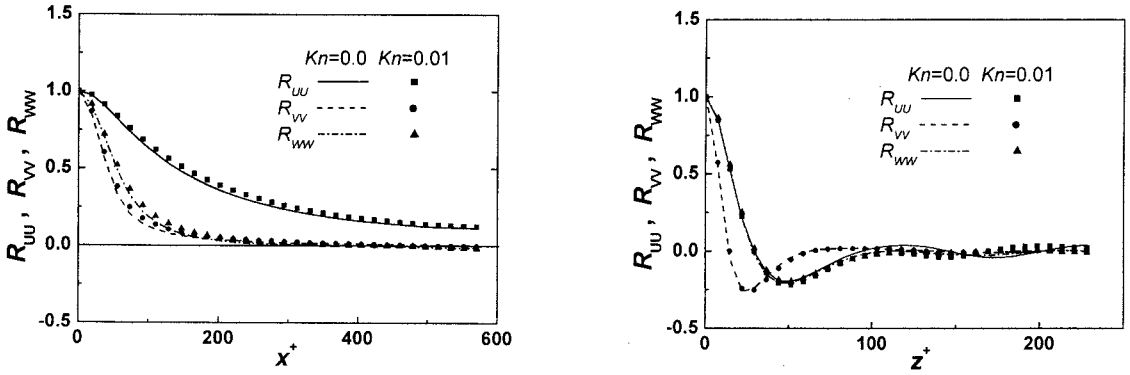

FIG. 2. Two-point correlation coefficients; (a) streamwise; (b) spanwise

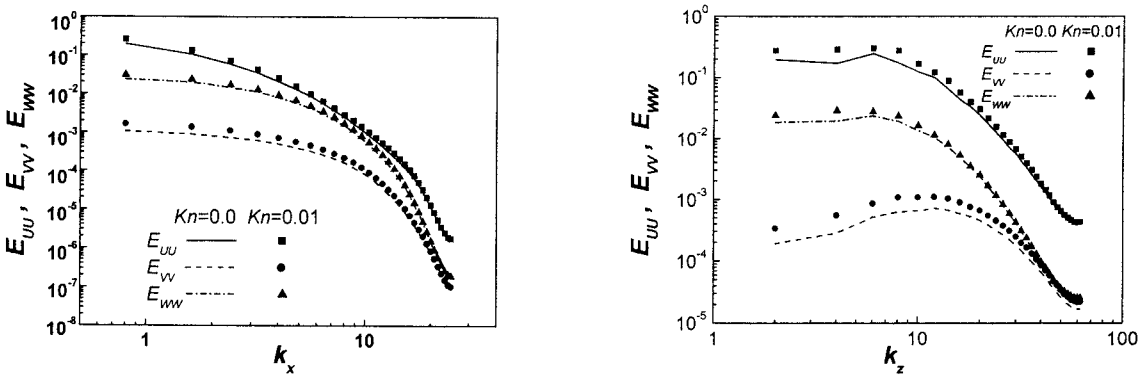

FIG. 3. One-dimensional energy spectra; (a) streamwise; (b) spanwise

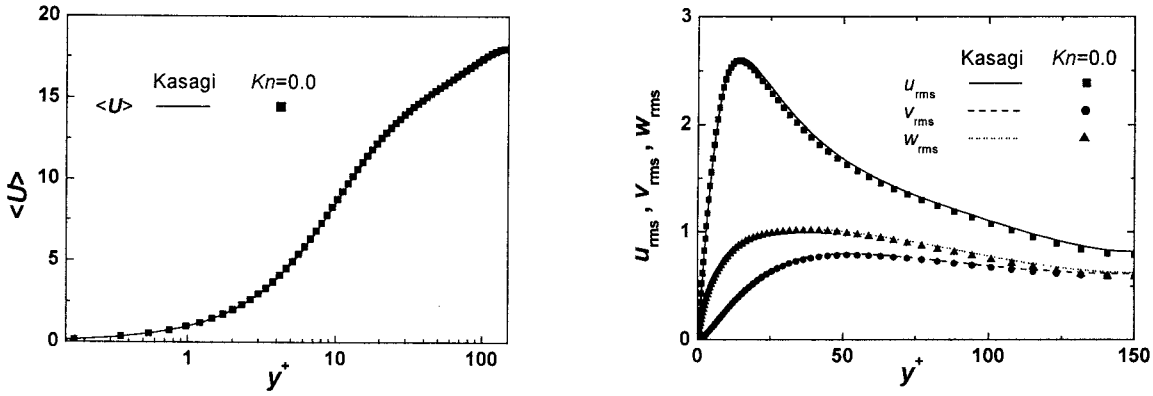

FIG.4 Comparison with the available database; (a) streamwise mean velocity; (b) turbulent intensities

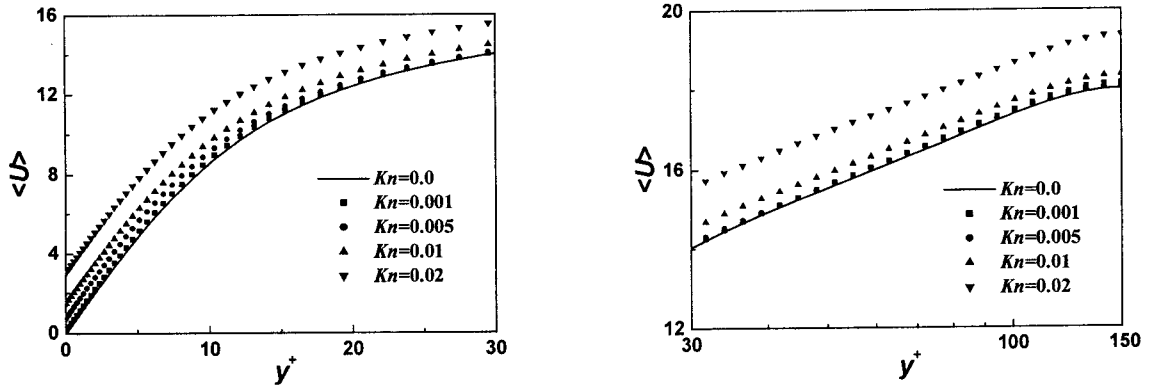

FIG. 5 Streamwise mean velocities under rarified conditions; (a) in the region of $0 \le y^+ < 30$; (b) in the region of $30 \le y^+ \le 150$

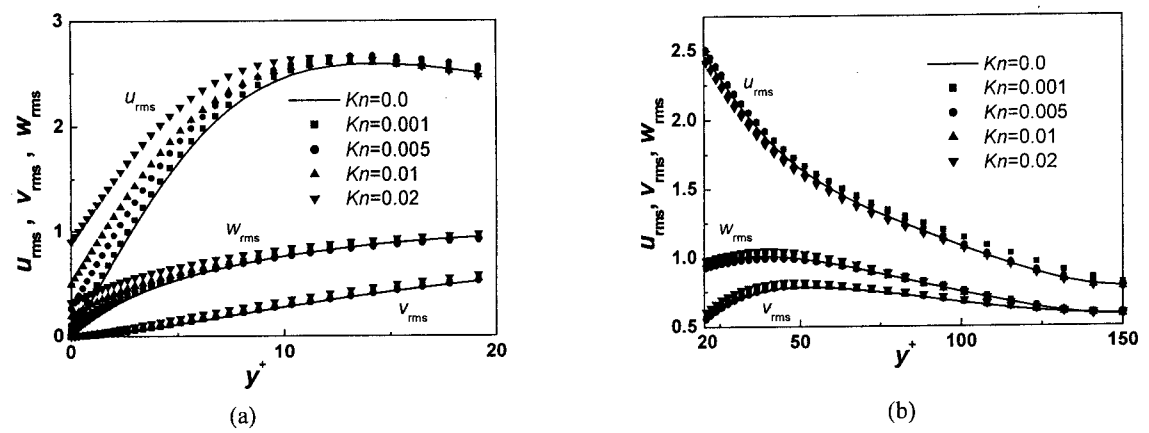

FIG. 6 Turbulent intensities under rarified conditions; (a) in the region of $0 \le y^+ < 20$; (b) in the region of $20 \le y^+ \le 150$

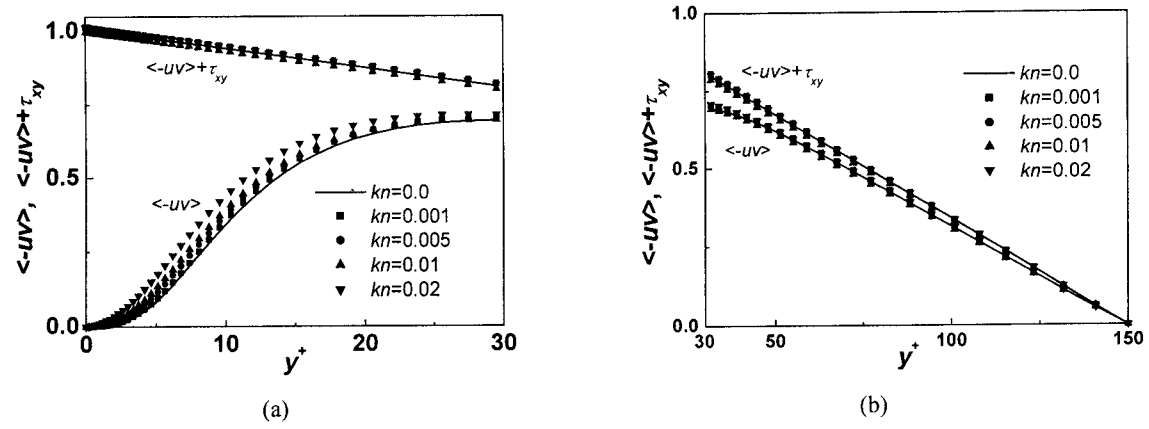

FIG. 7 Reynolds shear stress under rarified conditions; (a) in the region of $0 \le y^+ < 30$; (b) in the region of $30 \le y^+ \le 150$